JOURNAL OF APPLIED ELECTROCHEMISTRY 24 (1994) 1235–1243

Dynamic behaviour of an electrolyser with a two phase solid–liquid electrolyte
Part II: Investigation of elementary phenomena and electrode modelling

C. GABRIELLI, F. HUET, R. WIART, J. ZOPPAS-FERREIRA*

UPR15 du CNRS "Physique des Liquides et Electrochimie" Université Pierre et Marie Curie, Tour 22, 4 place Jussieu, 75252 Paris, Cedex 05, France

Received 17 December 1993; revised 13 April 1994

The dynamic behaviour of an electrolyser with a two phase solid–liquid electrolyte was investigated. In a previous paper some results were obtained with high particle concentrations by means of spectral analysis of the electrolyte resistance fluctuations and of the potential fluctuations. Here low bead concentrations were used. This allows potential and electrolyte resistance transients to be well separated and to be studied in the time domain. This analysis gives a detailed view of the approach and residence of the beads near the collector, and a quantitative estimation of the ohmic drop effect for insulating and conductive beads. Ohmic drop fluctuations account for the potential fluctuations for insulating glass beads. Zinc beads behave as insulating particles in the low frequency range and generate a similar ohmic drop effect. They behave as conducting particles in the high frequency range and the fast charge exchange induces depolarizing pulses which favour the formation of compact zinc deposits on the current collector. From the analysis of both transients and PSDs of the electrolyte resistance and potential fluctuations, the mean percentage of the particles colliding with the collector has been estimated even for high bead concentrations.

1. Introduction

In a previous paper [1], it was shown that the use of a simple electrolyser allows the electrochemical processes related to the collisions between metallic or insulating beads and the current collector in a two phase solid–liquid electrolyte to be analysed. Thanks to the simultaneous measurement of the power spectral densities (PSD) of the potential and electrolyte resistance fluctuations, the part due to the ohmic drop in the global potential fluctuations was evaluated. For glass beads and a current density i greater than $10\,\mathrm{mA\,cm^{-2}}$, the potential fluctuations are due to the ohmic drop fluctuations induced by the collisions of the beads onto the collector. For zinc beads the ohmic drop fluctuations contribute to the global potential fluctuations, but the potential fluctuations related to the electrical charge exchanges between the beads and the current collector play a significant role.

Modelling of the PSDs requires knowledge of the potential and electrolyte resistance elementary transients caused by collisions. For high bead concentrations [1], these transients overlapped and could not be extracted from the time recordings. Hence, the shape of spectra could not be explained and parameters such as the rate of collisions, or the rate of circulating beads were not derived.

In the present paper, by using very low concentration of beads ($\sim 10^{-2}\%$) the elementary phenomena will be separated and a thorough description of the processes will be proposed. Furthermore, this description will allow the dynamic behaviour of the two phase solid–liquid electrolyte to be more precisely analysed in practical conditions, i.e. for high bead concentrations.

2. Experimental results

2.1. *Potential and resistance fluctuations with glass beads*

The experimental arrangement was described in [1]. With a 0.08% glass bead concentration, the elementary events were recorded for an electrolyte velocity $v = 1.2\,\mathrm{m\,s^{-1}}$ and a high cathodic current density $120\,\mathrm{m\,A\,cm^{-2}}$ (Fig. 1). As expected, the $\Delta R_e(t)$ fluctuations were always positive, i.e. the electrolyte resistance increased in the presence of glass beads. In addition, the shape of the elementary transients in the $V-$ and R_e–time recordings were identical, except that they had an opposite sign. By multiplying $\Delta R_e(t)$ by the current value I ($I < 0$ for a cathodic current), the potential fluctuations $\Delta V(t)$ were found. This result, already reported in [1] for high

* Present address: LACOR/DEMAT/UFRGS, Av. Osvaldo Aranha, 99/706, 90210 Porto Alegre, RS Brasil.

0021-891X

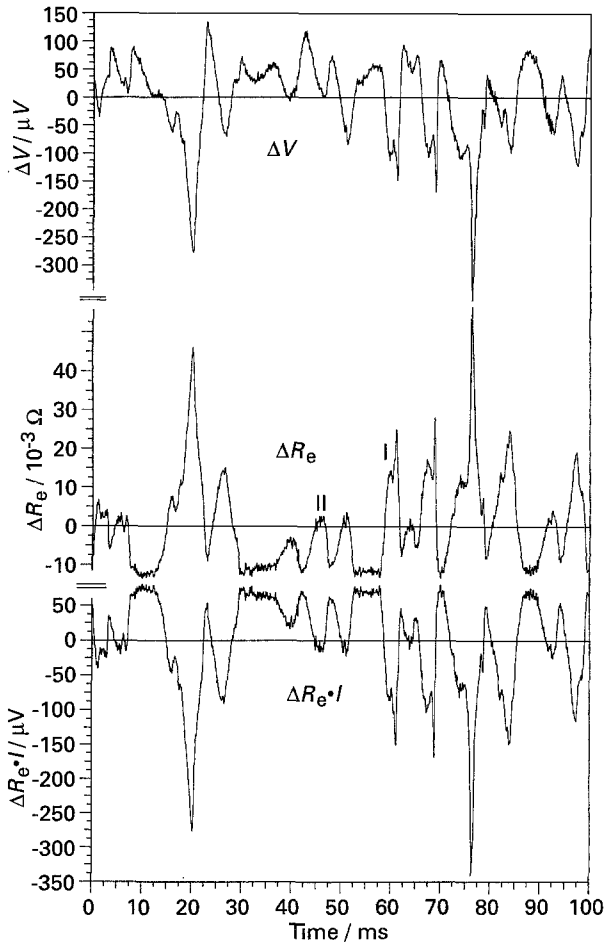

Fig. 1. Time recordings of the potential $\Delta V(t)$, electrolyte resistance $\Delta R_e(t)$, and ohmic drop $\Delta R_e I(t)$ fluctuations for a 0.08% glass bead concentration and a cathodic current density of 120 mA cm^{-2} ($\nu = 1.2$ m s^{-1}). Arbitrary origins.

glass bead concentrations, was a confirmation that the potential fluctuations $\Delta V(t)$ derived from ohmic drop, $I\Delta R_e(t)$, fluctuations for high current densities.

From these recordings, two typical shapes of transients (indicated by I and II in Fig. 1) were observed, depending on the perturbation produced by the glass beads. Two situations can be considered: (i) a bead hits the collector (transient I) or (ii) a bead goes near the collector without hitting it (transient II). In the two cases the bead provokes a perturbation of the primary current distribution, which gives rise to a change, ΔR_e, in the electrolyte resistance and then to a change, $\Delta V = I\Delta R_e$, in the ohmic drop. This relationship can also be checked on the PSD, as in [1] (Equation 4), even for a low bead concentration.

With the same bead concentration, the electrolyte velocity ν was changed (Fig. 2). The R_e transients were shorter and more frequent when the velocity increased, which gave an increase in the cut-off frequencies f_{c1}, f_{c2} on the corresponding PSD (Fig. 3). The high frequency plateau ($f > 500$ Hz) observed in curve (a) of Fig. 3 was due to the background noise of the electronic device.

The shape of the transients explains the two cut-off frequencies of the PSD. As will be seen later, the type II transient gives information about the passage time, between the reference electrode and the collector, of

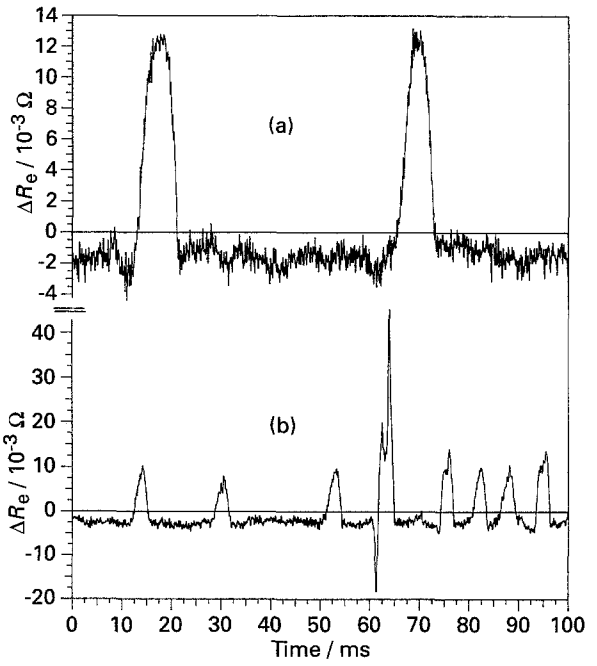

Fig. 2. R_e–time recordings for a 0.04% glass bead concentration (anodic current density of 40 mA cm^{-2}) and different electrolyte velocities: (a) $\nu = 0.7$ m s^{-1}, (b) $\nu = 2.2$ m s^{-1}. Arbitrary origins.

beads that do not hit the electrode, whereas the type I transient also gives information about the approach time of the beads very close to the collector.

The R_e transients show that the time required by a bead to go from the reference electrode to the collector is larger than the time spent by this bead very close to the collector (termed the residence time). Hence the displacement of the beads between the two electrodes corresponds to the transient with the longest time constant and is related to the low frequency part of the PSD (cut-off frequency f_{c1}). The residence time, associated with the second part of the type I transient, is shorter and related to the mid-frequency part of the PSD (cut-off frequency f_{c2}).

To diminish the probability of bead-collector collision, the electrode shape was changed. For a plane electrode, parallel to the electrolyte flow, the type I transients were very rare. The PSD showed that the low frequency plateau was not changed compared to the usual electrode, whereas the level of the plateau preceding the cut-off frequency f_{c2} decreased.

2.2. *Potential and resistance fluctuations with zinc beads*

With a 0.04% zinc bead concentration, the elementary events could be separated. Figure 4 gives the potential– and electrolyte resistance–time recordings for a low cathodic current density of 10 mA cm^{-2} and an electrolyte velocity of $\nu = 1.2$ m s^{-1}. As expected, the R_e transients showed a decrease in the electrolyte resistance when a zinc particle was near the electrode. The exact instants of the bead-collector collisions could be detected on the potential-time recordings which showed the depolarizing exponential transients characteristic of the electrical charge exchanges.

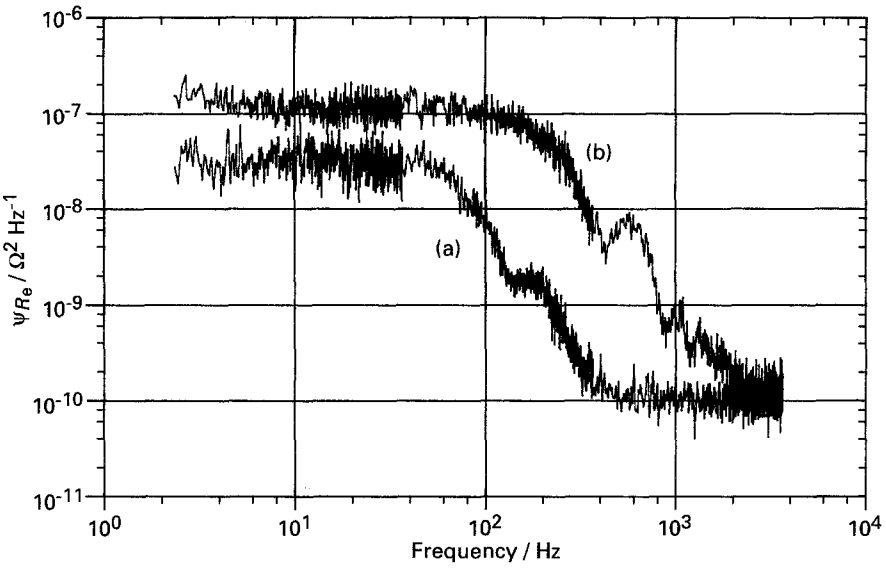

Fig. 3. PSDs corresponding to cases (a) and (b) in Fig. 2.

A comparison with Fig. 1 (glass beads) shows that the shape of the transient characteristic of the R_e fluctuations is the same for conducting or insulating beads, but with an opposite sign: the R_e fluctuations measured at 100 kHz are positive with glass beads and negative with zinc beads. The interpretation of the transient shape previously given for glass beads, i.e. the type I transient in Fig. 1 corresponds to the approach of a bead close to the collector followed by a contact, is now perfectly justified as the contact was detectable on the potential transient measured with zinc beads. When a type II transient appeared on the R_e–time recordings with zinc beads, there was no exponential decay in the V–time recording which confirmed the absence of collision.

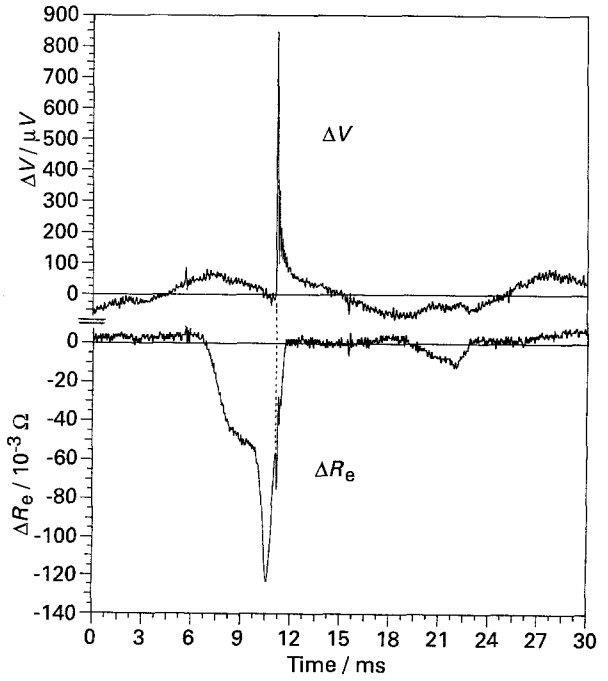

Fig. 4. Time recordings of the potential $\Delta V(t)$ and electrolyte resistance $\Delta R_e(t)$ fluctuations for a 0.04% zinc bead concentration at a cathodic current density of 10 mA cm^{-2} ($v = 1.2$ m s^{-1}). Arbitrary origins.

3. Discussion

3.1. *Fluctuations related to charge transfer*

The analysis of the collector potential fluctuations showed that the zinc bead-collector collisions provoked steep depolarizing potential changes followed by exponential decays with time constant depending on electrode polarization.

Potential–time recordings and corresponding PSDs are compared with impedance diagrams [1, 2] obtained at the same polarization. The cut-off frequency f_{c3} related to the time constant τ of the exponential decay of the elementary transients and the characteristic frequency of the capacitive loop attributed to the charge transfer have the same value. This indicates that f_{c3} and τ are related to charge transfer.

When a conducting bead, which is at rest potential in the electrolyte, hits the polarized collector, it takes electrical charge and then leaves the collector, which needs some time to be charged again by the current control device. Hence, this collision provokes a fluctuation of the collector potential which is anodic if the polarization is cathodic and vice versa.

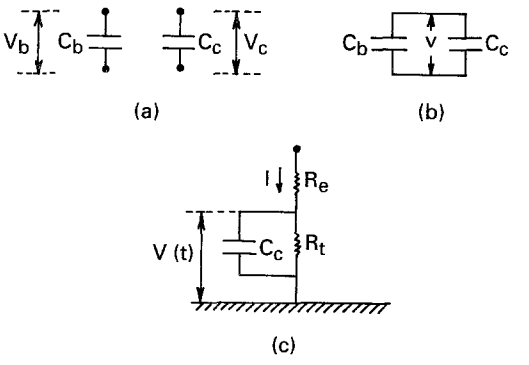

Fig. 5. Electrical scheme of the collector and a zinc bead before (a), during (b) and after (c) the collision.

3.1.1. Bead-collector collision. Figure 5 gives an electrical scheme for the collector and a zinc bead before (a), during (b) and after (c) the collision, which allows the potential V of the bead and collector during the collision to be calculated. For small changes in potential, the variation of the collector charge ΔQ_c due to the collision is related to the collector double layer capacity by

$$\Delta Q_c = C_c(V - V_c) \tag{1}$$

where V_c is the collector potential before the collision.

The same relationship may be written for the charge variation ΔQ_b of the bead. Thus,

$$\Delta Q_b = C_b(V - V_b) \tag{2}$$

where V_b is the bead potential before the collision.

The equation of the charge balance during the collision, $\Delta Q_c + \Delta Q_b = 0$, leads to the collector potential V:

$$V = \frac{C_c V_c + C_b V_b}{C_c + C_b} \tag{3}$$

which gives a collector potential jump, δV, given by

$$\delta V = V - V_c = \frac{C_b}{C_c + C_b}(V_b - V_c) \tag{4}$$

As beads and collector were zinc, they had the same capacity per unit surface. Hence,

$$\delta V = \frac{S_b}{S_c + S_b}(V_b - V_c) \tag{5}$$

For a collector area of $S_c = 0.05\,\text{cm}^2$ and a bead area of $S_b = 0.005\,\text{cm}^2$ (for a 400 μm diameter),

$$\delta V = 0.09(V_b - V_c) \tag{6}$$

The collector potential V_c can be obtained from the current–voltage curve (Fig. 2 in [1]) and V_b corresponds to the equilibrium potential of zinc in electrolyte ($V_b = E_0 = -1.575\,\text{V}$). As an example, for a $10\,\text{mA cm}^{-2}$ cathodic current, $V_c = -1.600\,\text{V}$ and $\delta V = +2.25\,\text{mV}$.

This value is in agreement with the average amplitude of the exponential transients of Fig. 8 in [1]. As the cathodic branch of the $I-V$ curve was almost vertical, V_c was practically constant, which explains that the transients had a current-independent average amplitude for current densities larger than $2\,\text{mA cm}^{-2}$. In addition, the decrease in the transient amplitudes with time can be associated with the potential V_c drift towards anodic potentials corresponding to a progressive electrode depolarization due to dissolution products of zinc beads [1, 2]. Similarly, for anodic polarization (exponential $I-V$ curve), Equation 6 leads to (i) negative jump amplitudes δV, (ii) larger amplitudes $|\delta V|$ for higher current polarization, in good agreement with the potential–time recordings. The random nature of the amplitudes of the observed transients can be explained by the various areas, S_b, of the zinc beads whose diameters ranged between 300 and 500 μm.

3.1.2. Collector recharging after collision. After collision the potential jump is sufficiently small to consider that the collector returns to its initial state by recharging the capacity C_c through the faradaic impedance. This process can be represented by the electrical scheme depicted in Fig. 5(c), where only the charge transfer resistance, R_t, is taken into account for the faradaic impedance, Z_F, as the time constant, τ, of the exponential transient is equal to the time constant, $R_t C_c$, of the charge transfer loop in the impedance diagram. Longer time constants would appear if the inductive loops of the faradaic impedance were included in Fig. 5(c). Therefore, restricting collector recharge to the fast exponential potential transient, probably leads to an incomplete recharge and allows the PSD Ψ_v to be explained only in the high frequency range.

After collision, the evolution of the collector charge, $Q_c(t)$, is given by

$$\frac{dQ_c}{dt} + \frac{Q_c}{R_t C_c} = I \tag{7}$$

where I is the controlled polarization current. Hence the collector potential variation $\delta V(t)$ is

$$\begin{aligned}\delta V(t) = V(t) - V(\infty) &= \frac{Q_c(t) - Q_c(\infty)}{C_c} \\ &= \frac{Q_c(0) - Q_c(\infty)}{C_c} e^{-t/R_t C_c} \\ &= \delta V\, e^{-t/R_t C_c}\end{aligned} \tag{8}$$

where the amplitude of the potential jump, δV, depends on the charge $Q_c(0) - Q_c(\infty)$ exchanged with the zinc particle, which is a function of the particle size. As the collisions were sufficiently separated in time (see Fig. 8 in [1]), the potential transients did not overlap and therefore could be summed; hence the collector potential fluctuations $\Delta V(t)$ may be written

$$\Delta V(t) = \sum_{i=1}^{N(t)} \delta V_i h(t - T_i) \tag{9}$$

where $N(t)$ is the number of transients between the initial time and time t, T_i and δV_i are the triggering time and the jump amplitude of the ith transient, respectively, and $h(t)$ is equal to

$$\begin{aligned} h(t) &= e^{-t/R_t C_c} \quad \text{if } t > 0 \\ &= 0 \qquad\qquad \text{if } t < 0 \end{aligned} \tag{10}$$

The PSD Ψ_v of the collector potential fluctuations can be calculated by means of the filtered Poisson process theory [3, 4]:

$$\Psi_v(f) = 2\lambda_c \langle \delta V^2 \rangle |H(f)|^2 \tag{11}$$

where λ_c is the number of collisions per unit time, $\langle \delta V^2 \rangle$ the average value of $(\delta V)^2$, and $H(f)$ the Fourier transform of $h(t)$:

$$H(f) = \int_{-\infty}^{+\infty} h(t)\, e^{-2j\pi ft} dt = \left(\frac{1}{R_t C_c} + 2j\pi f\right)^{-1}$$

Table 1. Characteristic parameters of the collector potential fluctuations induced by zinc beads in the cathodic domain ($\nu = 1.2\,m\,s^{-1}$)

i /mA cm^{-2}	*Beads* /%	$\langle\Delta V\rangle$ /mV	τ /μs	λ_c /s^{-1}	Ψ_{vo} /V^{2}Hz^{-1}	Ψ^*_{vo} /V^{2}Hz^{-1}
10	2	2.0	50	1200	2.4×10^{-11}	2.0×10^{-11}
20	2	2.5	32	1200	1.5×10^{-11}	1.6×10^{-11}
20	0.4	2.5	32	400	5.1×10^{-12}	6.0×10^{-12}
20	4	2.0	32	2600	2.1×10^{-11}	2.0×10^{-11}
1	4	0.9	50	2600	1.1×10^{-11}	1.0×10^{-11}

Hence,

$$\Psi_v(f) = \frac{2\lambda_c\langle\delta V^2\rangle\tau^2}{1 + 4\pi^2 f^2\tau^2} \tag{12}$$

with

$$\tau = R_t C_c \tag{13}$$

This PSD shows a plateau, Ψ_{vo}:

$$\Psi_{vo} = 2\lambda_c\langle\delta V^2\rangle\tau^2 \tag{14}$$

followed by a decrease in f^{-2}. In some cases this plateau was observed down to very low frequencies (Fig. 9, curve (a) in [1]); in other cases where the PSD Ψ_{Rel} of the ohmic drop fluctuations prevailed, this plateau was only seen at high frequencies (around 1 kHz in Fig. 9 curves (b) and (c) in [1]).

3.1.3. Comparison of experimental and theoretical PSD. Equation 12 shows that the cut-off frequency f_{c3} of the PSD Ψ_v gives the time constant τ of the exponential transients $\tau = 1/2\pi f_{c3}$. It was confirmed from the values of the charge transfer resistance R_t and the collector double layer capacity C_c given by the measured impedance diagram, that this time constant τ was equal to the product $R_t C_c$ in agreement with Equation 13.

To calculate the PSD, the estimation of the parameters $\langle\delta V^2\rangle$ and λ_c from the potential–time recordings is needed. $\langle\delta V^2\rangle$ can be obtained from the average $\langle\delta V\rangle$ of the potential jump amplitudes, over a large number of transients, by using the approximation

$$\langle\delta V^2\rangle = \langle\delta V\rangle^2 \tag{15}$$

which was verified within a 10% precision on the time recordings.

As an example, Table 1 gives for various experimental conditions the value Ψ_{vo} of the high frequency plateau (Equation 14) calculated from the values of $\langle\delta V\rangle$ and λ_c evaluated from the time recordings, and the value Ψ^*_{vo} obtained on the experimental PSD. Table 1 shows a good agreement between Ψ_{vo} and Ψ^*_{vo}, taking into account the measurement accuracy (22% for a PSD averaged over 20 elementary spectra). The same comparison was performed in the anodic domain and similar results were obtained.

3.1.4. Influence of zinc beads in zinc electrocrystallization. The effect of the zinc bead collisions with the cathodically polarized collector is mainly located at the conducting interfacial layer which plays a prominent role in the mechanism of zincate ion discharge. The kinetics of zinc electrocrystallization strongly depend on the layer properties: a semi-blocking and thick layer leads to irregular or spongy deposits whereas a conducting layer gives a more active electrode with compact deposits.

As shown in [1], the ADZ species in the electrolyte due to zinc bead dissolution induces heterogeneities in the conducting interfacial layer which destabilized the growth of compact deposits leading to nonadherent spongy deposits. This negative effect of the zinc beads was compensated by the zinc bead-electrode collisions which delayed the degeneration of compact deposits. This could not be explained by a mechanical effect of the collisions as, in an ADZ containing electrolyte, the degeneration was quicker with glass beads than without beads.

It is known that dendritic and spongy zinc deposits can be avoided with pulsed current techniques [5]. The current pulse duration must be short enough so as not to perturb the concentration profile. Slight zinc dissolution between the current pulses improves the deposit compactness.

Possibly, as for pulsed currents, the depolarizing potential jumps induced by zinc bead-electrode collisions lead to a more compact collector deposit, as they provoke local zinc dissolution or, at least, local decreases in the electrocrystallization rate.

3.2. *Fluctuations related to screening effects*

From the time recordings given in Figs 1–3, it was shown that the approach of conducting or insulating beads to the collector caused, by a screening effect, changes in the electrolyte resistance showing two time constants related to the approach time of beads between the reference and the working electrodes and to their residence time close to the collector.

3.2.1. Shape of the R_e transients. Although the shape of the transient was the same for both types of beads, its direction depended on the insulating or conducting nature of particles ($\Delta R_e > 0$ for glass beads and $\Delta R_e < 0$ for zinc beads). In addition, the mean value of the electrolyte resistance, R_e, measured with the electronic device referred to in [1] confirmed the results obtained with the electrochemical impedance technique, i.e. R_e increased with glass beads and decreased with zinc beads.

From Figs 1–4, the distance x to the collector from which the beads began to influence the electrolyte resistance can be estimated, using

$$x = T_t\nu \tag{16}$$

where T_t is the transient life time and ν the electrolyte velocity. Experimental typical T_t values measured for different velocities were in the 4–6 ms range, yielding x values between 0.48 and 0.72 cm. These values fitted fairly well with the distance between the potential probe and the collector.

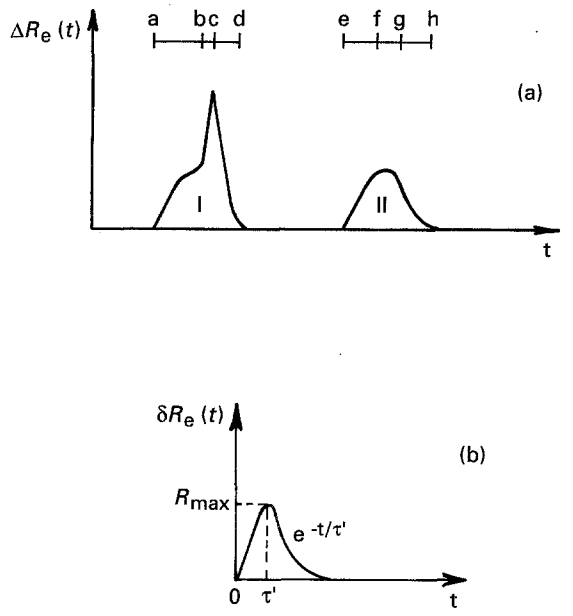

Fig. 6. Scheme of the elementary electrolyte resistance transients provoked by the presence of glass beads: (a) definition of the various parts, (b) linear exponential transient.

Figure 6(a) shows the two shapes of transients generated by glass beads. The measured electrolyte resistance began to be influenced by a bead when it passed at the reference electrode level (point *a* in Fig. 6(a)). The primary current lines were perturbed and the electrolyte resistance increased as the glass bead proceeded towards the collector (segment *ab*). Very close to the electrode the potential field was more modified and ΔR_e reached its maximum value (point *c*); then ΔR_e decreased as soon as the bead moved away from the collector (segment *cd*). The approach time (segment *ab*) and the residence time very close to the collector (segment *bc*) can therefore be estimated. Given the electrolyser geometry, a bead could pass in front of the electrode at such a distance that it did not provoke the perturbation corresponding to segment *bc* in the type I transient. In this case, the type II transient appeared and three times could be distinguished: the approach time (*ef*), the passage time in front of the collector (*fg*) and the removal time (*gh*).

Hence the shapes of the R_e transients can be explained by considering that the electrolyte resistance has two components: R_{e1} related to the electrolyte resistance in the channel (between the reference and working electrodes) and R_{e2} related to the electrolyte/metal interface (which concerns a zone close to the collector). The type II transients give information on the $\Delta R_{e1}(t)$ fluctuations and the type I transients on both $\Delta R_{e1}(t)$ (segment *ab*) and $\Delta R_{e2}(t)$ (segment *bd*) fluctuations.

The average characteristic times and the corresponding distances, obtained from the R_e–time recordings, for an electrolyte velocity $v = 1.2\,m\,s^{-1}$, are given in Table 2. The same results were found for glass or zinc beads, as they had approximately the same size and density. In contrast, the transient amplitudes were always larger with zinc beads, as discussed later.

Table 2. Characteristic parameters defined in Fig. 6(a) and deduced from the R_e time recordings ($v = 1.2\,m\,s^{-1}$)

Segment	*Time*/ms	*Distance*/mm
ab	3.1	3.7
bc	0.58	0.7
cd	1.33	1.6
ef	2.5	3.0
fg	1.67	2.0
gh	1.67	2.0

From the comparison of the R_e– and V–time recordings obtained with zinc beads (Fig. 4), the instants of the bead-collector collisions were shown to be located either at point *c*, or in the segment *cd* in Fig. 6(a). It was observed that the exact collision times could occur a few 10^{-4} s after the ΔR_e minima (Fig. 4); on the R_e–time recording the charge exchange was indicated by a small wiggle in the *cd* segment. Hence beads could approach very close to the electrode, move away from it and come back again under the effect of local turbulence. However, all the electrical charge exchanges between the metallic beads and the collector were systematically preceded by type I transients on the R_e time recordings.

3.2.2. Estimation of parameters. If the shape of the elementary R_e transient is known, the PSD of the electrolyte resistance fluctuations can be calculated and the number of beads which pass in front of the collector per unit time, λ_p, can be estimated from the experimental PSD.

As already noted, the common part of type I and II transients, which represents the approach of the bead from the reference electrode to the collector is related to the low frequency plateau in the PSD of the R_e fluctuations. For λ_p estimation, the upper part of the type I transient (segment *bc*), which corresponds to the midfrequency plateau of the PSD, may be ignored. Then all transients are considered to have a linear-exponential shape (Fig. 6(b)), such that

$$\delta R_e(t) = \frac{e R_{max}}{\tau'} t\, e^{-t/\tau'} \quad \text{if } t > 0$$
$$= 0 \quad \text{if } t < 0 \qquad (17)$$

where R_{max} and τ' are the amplitude and the time constant, respectively, and e = 2.718. This shape is sufficiently close to that of the experimental transients for glass beads and allows the analytical solution to be derived. This derivation is also valid for zinc beads as only the sign of the R_e transient changes.

As the elementary events generated by the passage of the beads in front of the collector were independent, the triggering times T_i of these events followed a Poisson process. For calculating the PSD of the R_e fluctuations, it is assumed that the $\Delta R_e(t)$ variations were additive:

$$\Delta R_e(t) = \sum_{i=1}^{N(t)} \delta R_e(t - T_i) \qquad (18)$$

Table 3. Characteristic parameters of the $\Delta R_e(t)$ fluctuations induced by glass beads

ν /m s^{-1}	*Beads* /%	$\Psi_{Re}(0)$ /Ω^2Hz^{-1}	f_{cl} /Hz	τ' /s	$\langle R_{max}\rangle \pm 0.005$ /Ω	λ_p /s^{-1}
1.2	0.08	7.8×10^{-7}	170	9.3×10^{-4}	0.02	1.5×10^{2}
1.2	0.4	6.9×10^{-6}	170	9.3×10^{-4}	0.02	1.3×10^{3}
1.2	2	2.8×10^{-5}	170	9.3×10^{-4}	0.02	5.5×10^{3}
1.2	4	5.6×10^{-5}	170	9.3×10^{-4}	0.02	1.1×10^{4}
2.2	4	5.6×10^{-5}	235	6.8×10^{-4}	0.02	2.0×10^{4}

where $N(t)$ is the number of transients occurring between the initial instant and time t, T_i the triggering time of the ith transient. This approximation is less valid when the bead concentration increases. As for potential fluctuations, the filtered Poisson process theory gives the PSD of the R_e fluctuations:

$$\Psi_{Re}(f) = 2\lambda_p \langle |R(f)|^2 \rangle_{R_{max}} \tag{19}$$

where $R(f)$ is the Fourier transform of the elementary transient $\delta R_e(t)$ and $\langle\ \rangle_{R_{max}}$ means average value over R_{max} which can be shown to be a random quantity in Figs 1 and 2:

$$R(f) = \int_{-\infty}^{\infty} \delta R_e(t)\, e^{-j2\pi ft} dt = \frac{e R_{max} \tau'}{(1 + 2j\pi f\tau')^2} \tag{20}$$

Hence:

$$\Psi_{Re}(f) = 2\lambda_p e^2 \langle R_{max}^2 \rangle \frac{\tau'^2}{(1 + 4\pi^2 f^2 \tau'^2)^2} \tag{21}$$

This PSD shows a low frequency plateau, such that

$$\Psi_{Re}(0) = 2\lambda_p e^2 \langle R_{max}^2 \rangle \tau'^2 \tag{22}$$

followed by a $1/f^4$ decrease in the high frequency range. The cut-off frequency,

$$f_{cl} = \frac{1}{2\pi\tau'} \tag{23}$$

can be obtained from the PSD level,

$$\Psi_{Re}(f_{cl}) = \frac{\Psi_{Re}(0)}{4} \tag{24}$$

The parameters λ_p, $\langle R_{max}\rangle$ and τ' can be estimated from the experimental R_e–time recordings and PSD. First, the R_e–time recordings obtained at low bead concentrations give a mean value of R_{max}. Second, the experimental PSD always shows two plateaux, but only the low frequency plateau followed by the $1/f^4$ decrease must be considered for λ_p and τ' determination. As already stated, this part of the spectrum was not influenced by the variations of the R_{e2} component due to the approach of the beads close to the collector. The time constant τ' can be evaluated from the cut-off frequency f_{cl} (Equation 23) and the number of beads flowing through the channel per unit time, λ_p, can be estimated from the value of $\Psi_{Re}(0)$ under the same assumption as for the potential fluctuations:

$$\langle R_{max}^2 \rangle = \langle R_{max} \rangle^2 \tag{25}$$

The results are successively given for various concentrations of glass and zinc beads.

(a) Case of glass beads: Table 3 gives the characteristic parameters of the $\Delta R_e(t)$ fluctuations for high and low concentrations of glass beads. Another estimation of λ_p can be obtained by counting the transients on the R_e–time recordings corresponding to low bead concentrations; e.g. for a 0.08% concentration of glass beads flowing at 1.2 m s^{-1}, λ_p was equal to 150 beads s^{-1}, which is in good agreement with the value obtained in Table 3 from the PSD.

However, for a higher concentration, counting the transients was impossible as they overlapped. In this case, λ_p can be estimated from the electrolyte velocity, ν, and the bead concentration, c, by

$$\lambda_p = \frac{\pi d^2}{4} \nu c \tag{26}$$

where d is the channel diameter.

For a bead diameter, d_b, close to 300 μm, a bead density, ρ, of 2.7 g cm^{-3} and a mass, m, of beads introduced in a volume $\mathscr{U}_s = 250$ cm^3 of electrolyte, the bead concentration c in cm^{-3}, can be calculated by

$$c = \frac{6m}{\pi \rho d_b^3 \mathscr{U}_s} \tag{27}$$

Table 4 gives the values of c and λ_p estimated with Equations 26 and 27 for the various situations investigated.

A comparison of λ_p in Tables 3 and 4 shows good agreement within 25% precision. The estimation of λ_p in Table 4 assumes that all the beads added to the electrolyte passed in front of the collector. However, experimental observations revealed that some beads accumulated at various points in the electrolyser, especially near the Nylon cloth which enveloped the counter electrode. This may explain the lower values of λ_p deduced from the experimental PSDs (Table 3).

Table 4. Concentration and number of circulating particles per unit time calculated with Equations 26 and 27

ν /m s^{-1}	*Beads* /%	m /g	c /beads cm^{-3}	λ_p /s^{-1}
1.2	0.08	0.3	30	2.5×10^{2}
1.2	0.4	1.5	1.6×10^{2}	1.3×10^{3}
1.2	2	7.5	8.0×10^{2}	6.8×10^{3}
1.2	4	15	1.6×10^{3}	1.4×10^{4}
2.2	4	15	1.6×10^{3}	2.5×10^{4}

Table 5. Characteristic parameters of the $\Delta R_e(t)$ fluctuations induced by zinc beads

ν /m s^{-1}	*Beads* /%	$\Psi_{Re}(0)$ /Ω^2 Hz^{-1}	f_{cl} /Hz	τ' /s	$\langle R_{max}\rangle \pm 0.003$ /Ω	λ_p *Eq. 22* /s^{-1}	λ_p *Eq. 26* /s^{-1}
1.2	2	3.1×10^{-4}	170	9.3×10^{-4}	0.07	4.9×10^3	1.4×10^3 -6.8×10^3

(b) Case of zinc beads: As an example, Table 5 gives the characteristic parameters of the $\Delta R_e(t)$ fluctuations for a 2% zinc bead concentration. The first value of λ_p is calculated from the experimental PSD (Equation 22) with a $\langle R_{max}\rangle$ value estimated from R_e–time recordings measured for a low bead concentration (0.08%). Two extreme values of λ_p evaluated from the bead concentration and the electrolyte velocity (Equation 26) are also given in Table 5; they correspond to the minimum (300 μm) and maximum (500 μm) diameters of the zinc beads. It can be seen that, first, the λ_p values are in agreement, and, second, the λ_p values for zinc beads and glass beads fit well.

A difference can be noticed between the values of $\langle R_{max}\rangle$ obtained experimentally with glass beads (Table 3) and zinc beads (Table 5). The decrease in the electrolyte resistance induced by a conducting bead was equal, on average, to 3.5 times the R_e increase due to an insulating bead. This is in agreement with the PSD levels of Figs 6 and 10 in [1]: Ψ_{Re} was 10 times smaller for glass beads than for zinc beads.

The potential–time recordings allow the number λ_c of beads hitting the collector per unit time to be estimated (Table 1). The ratio λ_c/λ_p which represents the percentage of beads charged on the collector can then be evaluated. Table 6 shows that this ratio decreased when the bead concentration increased and was constant above a critical concentration.

Now the contribution of the ohmic drop fluctuations to the total potential fluctuations is discussed for zinc beads at high current densities; it was shown in Fig. 10 of [1] (and in Fig. 6(b) of [6]) that the PSDs Ψ_v and Ψ_{ReI} did not fit well, i.e. $\Delta V(t)$ was not equal to $\Delta R_e I(t)$ in the time domain.

Figure 7 shows V– and R_e–time recordings for a 0.08% zinc bead concentration at a cathodic current density of 120 mA cm^{-2}. For a negative current I, the ohmic drop $\Delta R_e I(t)$ variation should lead to a depolarizing transient which was not visible on $V(t)$. In contrast, an overpolarization similar to the ohmic drop change caused by an insulating particle, preceded the fast depolarizing transient due to the charge exchange. Therefore the electrolyte resistance variation measured at 100 kHz gave only qualitative information (shape, timing) for metallic particles as they behaved differently at high and low frequencies. At 100 kHz zinc beads were conductive (because of the presence of the double layer) and increased the global conductivity of the electrolyte; at low frequencies they behaved as insulating beads as they were at equilibrium potential so that no current flowed through them; therefore they decreased the electrolyte conductivity.

Table 6. Ratio λ_c/λ_p against the zinc bead concentrations

Beads/%	λ_c/λ_p
0.08	0.8
0.4	0.3
2	0.23
4	0.23

The discrepancy found in Fig. 10 of [1] can now be explained. At high current densities, the PSD Ψ_v should be explained by the charge exchange transients in the high frequency range and by the ohmic drop fluctuations in the low frequency range. Since zinc beads behaved as insulating beads at low frequencies, $\Psi_{v,zinc}$ must be compared with $\Psi_{ReI,glass}$. As an example, for a current density of 20 mA cm^{-2}

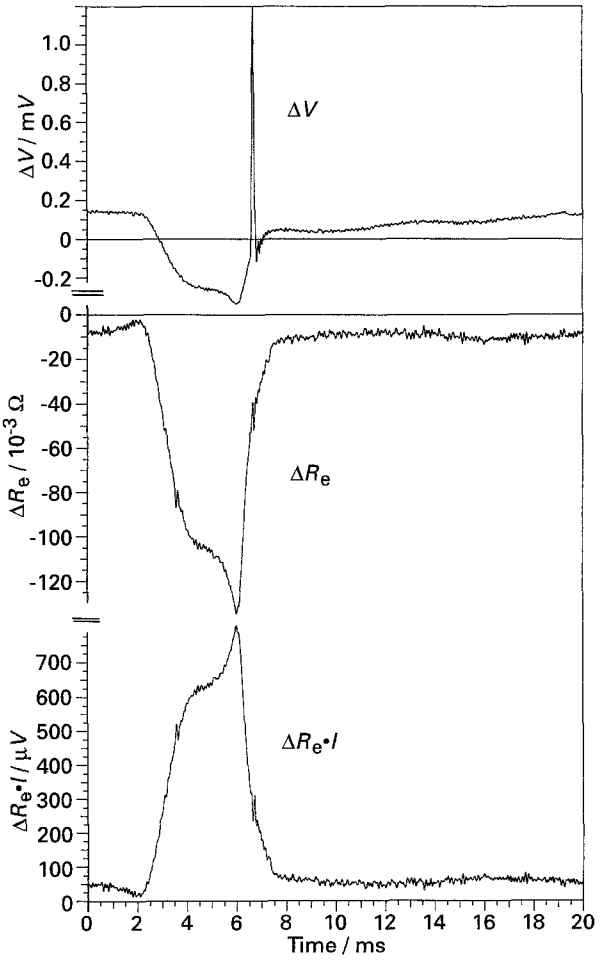

Fig. 7. Time recordings of the potential $\Delta V(t)$, electrolyte resistance $\Delta R_e(t)$, and ohmic drop $I\Delta R_e(t)$ fluctuations for a 0.08% zinc bead concentration and a cathodic current density of 120 mA cm^{-2} ($\nu = 1.2$ m s^{-1}). Arbitrary origins.

($I = 1\,\text{mA}$) Fig. 10 in [1] gives $\Psi_{v,\text{zinc}}(0) = 1.4 \times 10^{-10}\,\text{V}^2\,\text{Hz}^{-1}$ corresponding to ohmic drop fluctuations of insulating beads with a PSD $\Psi_{\text{Re,insul.}}$ such that

$$\Psi_{\text{Re,insul}}(0) = \frac{\Psi_{v,\text{zinc}}(0)}{I^2} = 1.4 \times 10^{-4}\Omega^2\,\text{Hz}^{-1}$$

Comparing this value with $\Psi_{\text{Re,glass}}(0) = 4.2 \times 10^{-5}\Omega^2\,\text{Hz}^{-1}$, given by Fig. 8 in [1], indicates that the ohmic drop fluctuations induced by insulating beads which would explain the potential fluctuations due to zinc beads, are three times larger than the ohmic drop fluctuations due to glass beads. However the mean ratio of the zinc and glass bead diameters was $d_z/d_g = 1.3$ (see Table 1 in [1]). Hence if the electrolyte resistance variation due to a bead is caused by a surface screening effect, the ratio of the mean amplitudes $\langle R_{\max} \rangle$ of the R_e transients for zinc and glass beads is equal to $(d_z/d_g)^2$, and the ratio of the PSD $\Psi_{Re}(0)$ to $(d_z/d_g)^4 \approx 3$, from Equation 22. Therefore, for zinc beads, the potential fluctuations at low frequencies may also be explained by ohmic drop fluctuations at high current densities, as for glass beads. At lower current densities the potential fluctuations were not controlled by ohmic effects as for glass beads.

4. Conclusion

For insulating particles, good separation between ohmic drop fluctuations and potential fluctuations due to other causes can be achieved by a simultaneous measurement of the electrolyte resistance fluctuations and the potential fluctuations. Therefore this technique may be very useful for two phase-flow systems [6] with insulating nonliquid phase (gas evolving electrode, electrolyser with insulating particles ...). For conductive beads this technique leads to qualitative results on the ohmic drop fluctuations. By using, as a reference, insulating beads of the same geometry, quantitative results can also be obtained.

By using low bead concentrations in the electrolyser, the electrolyte resistance transients were separated. The analysis of these transients gives a detailed picture of the approach of the beads to the collector and a quantitative estimation of the ohmic drop effect for insulating beads. Furthermore it allowed a modelling of the PSDs of the potential and electrolyte resistance fluctuations, which gave a way of estimating the characteristic parameters of the electrolyser, such as the mean numbers λ_c, λ_p of particles circulating and hitting the collector per unit time, the time constants τ, τ' involved in the V and R_e transients, even for high zinc bead concentrations.

From both frequency and time analyses, the potential fluctuations were confirmed to be ohmic drop fluctuations for glass beads for current densities higher than $10\,\text{mA}\,\text{cm}^{-2}$. For zinc beads, they were attributed to ohmic drop effects at low frequencies and to electrical charge exchanges between the collector and the beads at high frequencies. The fast depolarizing potential transients hinder the formation of a porous layer on the collector surface leading to compact zinc deposits.

References

[1] C. Gabrielli, F. Huet, R. Wiart and J. Zoppas-Ferreira, *J. Appl. Electrochem.*, submitted.
[2] J. Zoppas-Ferreira, PhD thesis, Université Paris V, France (1991).
[3] A. Papoulis, Probability, Random Variables and Stochastic Processes, ed. McGraw-Hill, New York (1965).
[4] C. Gabrielli, F. Huet, M. Keddam and R. Oltra, *in* 'Advances in Localized Corrosion' (edited by H. S. Isaacs, U. Bertocci, J. Kruger, S. Smialowska), NACE, Houston (1990) p. 93.
[5] E. D. Woumfo and O. Vittori, *J. Appl. Electrochem.* **21** (1991) 77.
[6] C. Gabrielli and F. Huet, *J. Appl. Electrochem.*, **24** (1994) 593.